Supplementary Information for:

The midbody interactome reveals new unexpected roles for PP1 phosphatases in cytokinesis

Luisa Capalbo[1], Zuni I. Bassi[1], Marco Geymonat[2], Sofia Todesca[1], Liviu Copoiu[1†], Anton Enright[1], Giuliano Callaini[3], Maria Giovanna Riparbelli[4], Lu Yu[5], Jyoti Choudhary[5≠], Enrico Ferrero[2,6#], Sally Wheatley[7], Max E. Douglas[8], Masanori Mishima[8,9] and Pier Paolo D'Avino[1*]

[1]Department of Pathology, University of Cambridge, Tennis Court Road, Cambridge, CB2 1QP, UK

[2]Department of Genetics, University of Cambridge, Downing Street, Cambridge, CB2 3EH, UK

[3]Department of Medical Biotechnologies and [4]Department of Life Sciences, University of Siena, Via A. Moro 4, 53100 Siena, Italy

[5]The Wellcome Trust Sanger Institute, Wellcome Genome Campus, Hinxton, CB10 1SA, UK

[6]Cambridge Systems Biology Centre, University of Cambridge, Tennis Court Road, Cambridge, CB2 1QR, UK

[7]School of Life Sciences, University of Nottingham, Nottingham. NG7 2UH.

[8]Wellcome Trust/Cancer Research UK Gurdon Institute, Cambridge CB2 1QN, UK

[9]Centre for Mechanochemical Cell Biology and Division of Biomedical Sciences, Warwick Medical School, University of Warwick, Coventry, CV4 7AL, UK.

This file includes:

Supplementary Figs. S1 to S5
Supplementary Tables S1 and S2
Captions for Supplementary Videos S1 to S8
Captions for Supplementary Data S1 to S5

Other Supplementary Information for this manuscript include the following:

Movies S1 to S8
Data S1 to S5

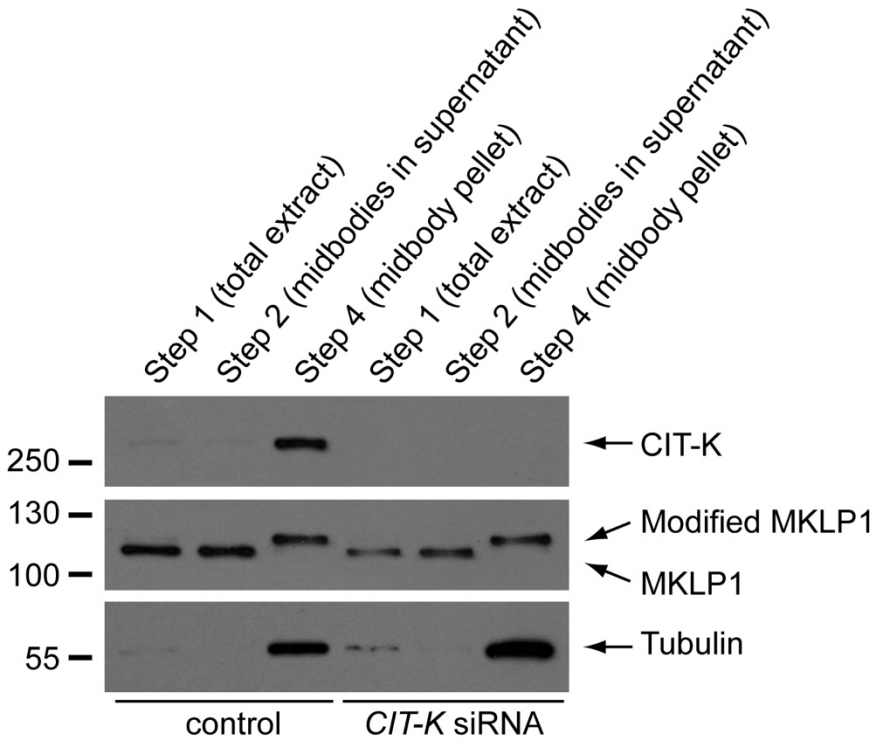

Supplementary Fig. S1. Purified midbodies are enriched for known midbody proteins. HeLa cells treated with siRNAs directed against either a random sequence (control) or *CIT-K* were synchronized in telophase to purify midbodies and aliquots from the different purification steps (see Materials and Methods) were analyzed by Western blot to detect CIT-K, MKLP1 and tubulin. The numbers on the left indicate the sizes in kDa of the molecular mass marker. Note that the slower migrating band detected with the anti-MKLP1 antibody is very likely a post-translational modified form of MKLP1.

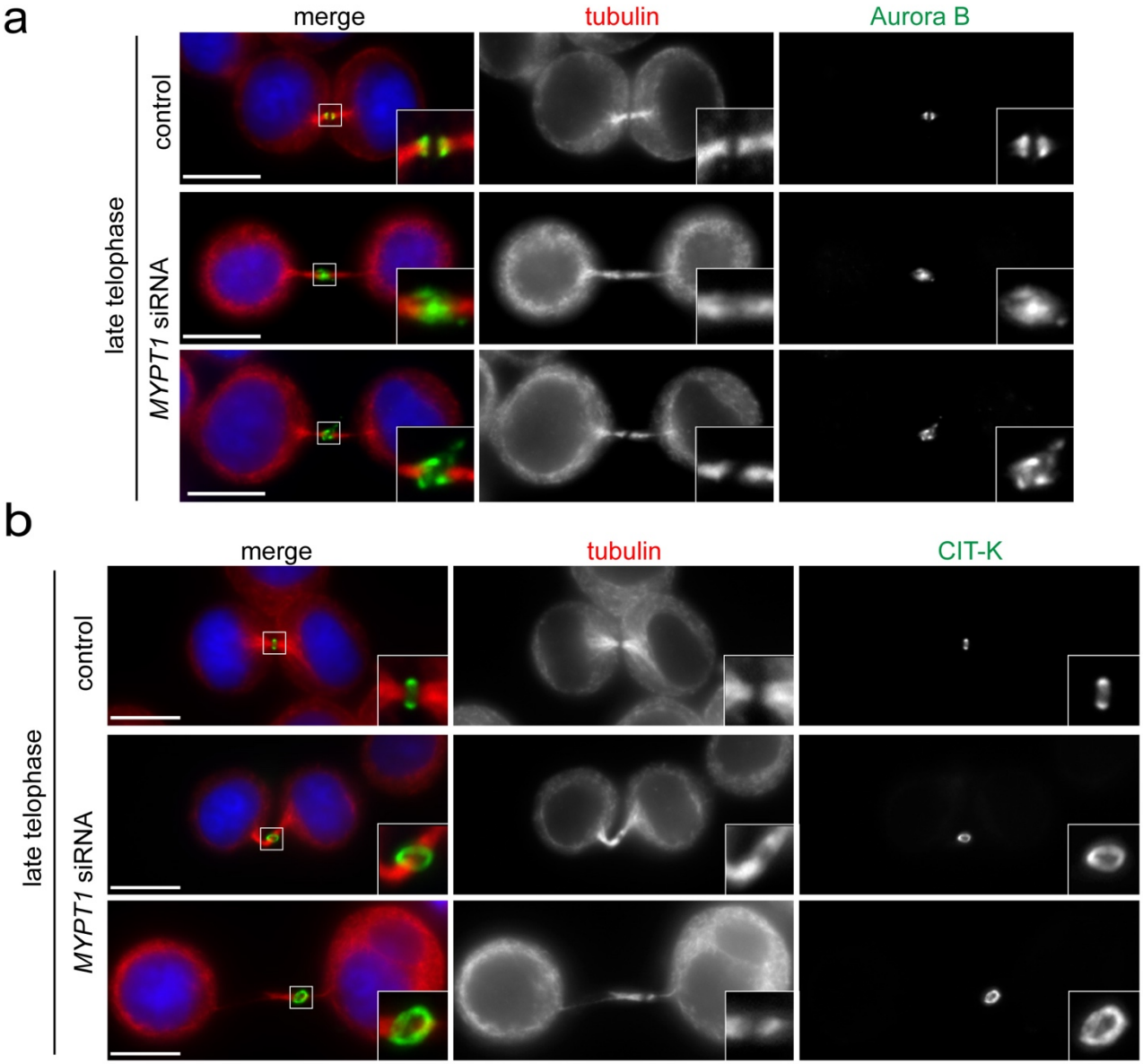

Supplementary Fig. S2. Analysis of cytokinesis defects after MYPT1 depletion in HeLa S3 cells. (a-b) HeLa S3 cells were treated with siRNAs directed against either a random sequence (control) or *MYPT1* and after 48 hours were fixed and stained to detect DNA (blue in the merged panels), tubulin, and either Aurora B (a) or CIT-K (b). DNA condensation and the shape and thickness of microtubule bundles at the intercellular bridge were used as criteria to stage telophase cells. Insets show a 3x magnification of the midbody. Bars, 10 µm.

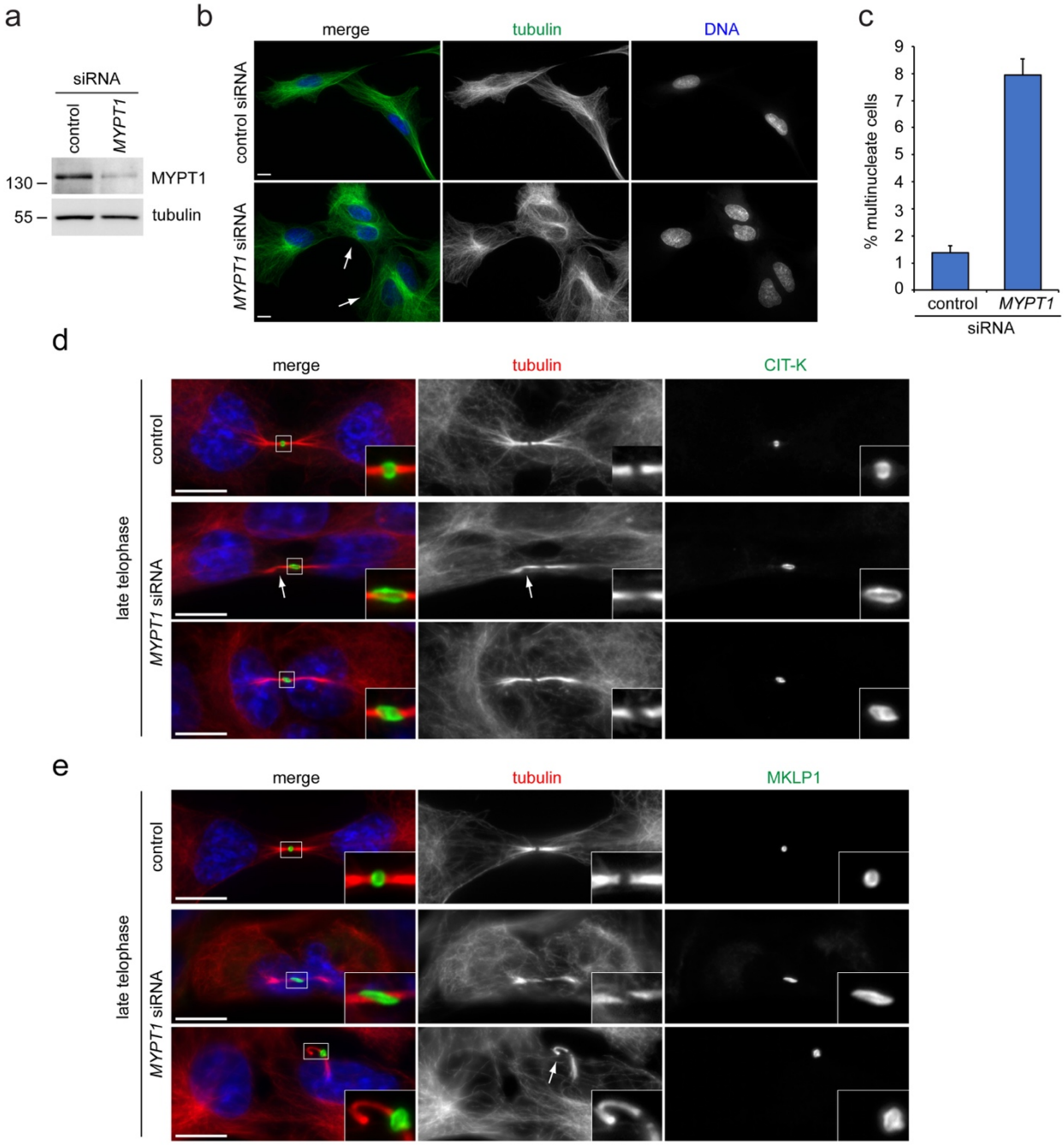

Supplementary Fig. S3. Analysis of cytokinesis defects after MYPT1 depletion in RPE-1 cells. (a) RPE-1 cells were treated with siRNAs directed against either a random sequence (control) or MYPT1 and after 48 h proteins were extracted and analyzed by western blot to detect the indicated proteins. The numbers on the left indicate the sizes in kDa of the molecular mass marker. (b) RPE-1 cells were treated with siRNAs directed against either a random sequence (control) or *MYPT1* and after 48 hours were fixed and stained to detect DNA and tubulin. The arrows indicate multinucleate cells. Bars, 10 µm. (c) Quantification of multinucleate cells obtained after control or MYPT1 siRNA. More than 700 cells were counted in each experiment, n=3. Bars indicate standard errors. (d-e) RPE-1 cells were treated with control or *MYPT1* siRNAs and after 48 hours were fixed and stained to detect the indicated epitopes and DNA (blue in the merged panels). DNA condensation and the shape and thickness of microtubule bundles at the intercellular bridge were used as criteria to stage telophase cells. Insets show a 3x magnification of the midbody. The arrows mark a bent (d) and a broken (e) central spindle, phenotypes that are very similar to those observed in HeLa cells (Fig. 6). Bars, 10 µm.

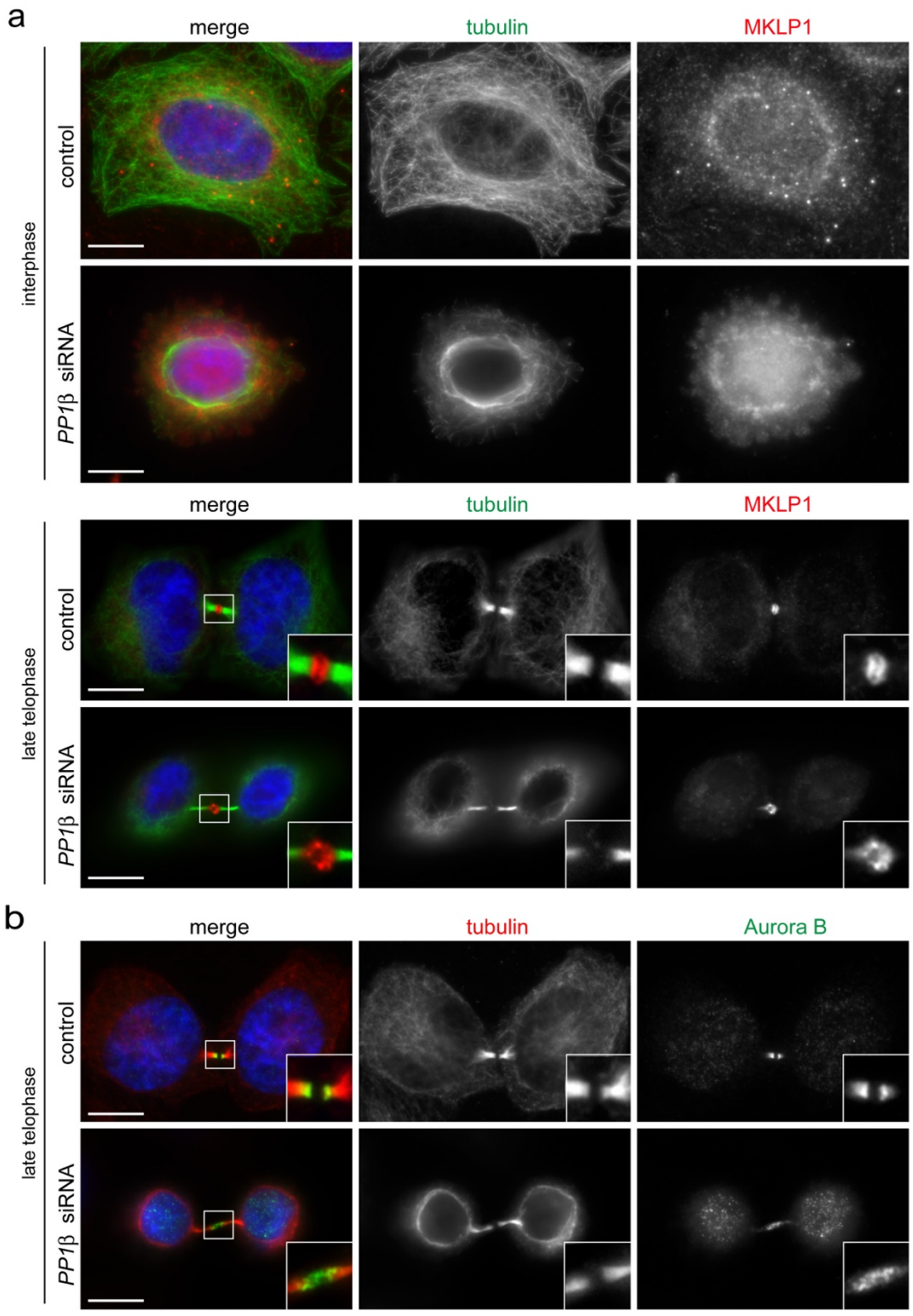

Supplementary Fig. S4. *PP1β* siRNA phenocopies MYPT1 depletion. (a-b) HeLa Kyoto cells were treated with siRNAs directed against either a random sequence (control) or *PP1β* and after 48 hours were fixed and stained to detect DNA (blue in the merged panels), tubulin and either MKLP1 (a) or Aurora B (b). DNA condensation and the shape and thickness of microtubule bundles at the intercellular bridge were used as criteria to stage telophase cells. Insets show a 3x magnification of the midbody. Bars, 10 µm.

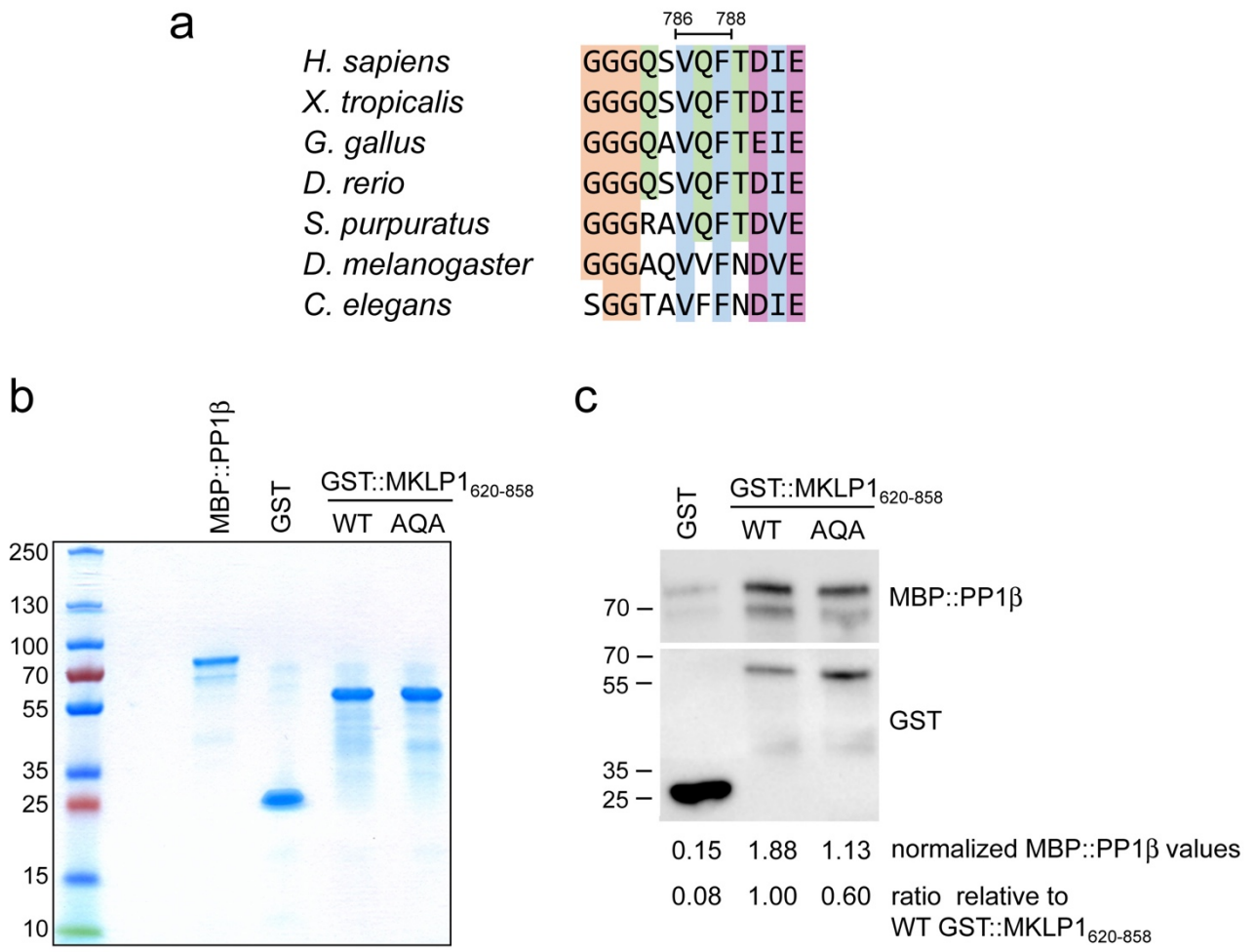

Supplementary Fig. S5. PP1β interacts with a conserved binding site in the MKLP1 C-terminus. (a) The amino acid sequences containing the PP1β binding site (aa 786-788) of human MKLP1 and its orthologues in other vertebrate and invertebrate species were aligned using the Muscle algorithm[1]. Amino acids are colored according to their chemical properties. (b) Coomassie-stained gel showing the purified proteins used in the GST pull down assay. (c) GST-tagged wild type and AQA mutant MKLP1 fragments (aa 620-858) were expressed and purified in bacteria and then employed in a pull down assay with MBP**::** PP1β purified from yeast. Proteins were then analyzed by Western blot using antibodies against MBP (top) and GST (bottom). At the bottom are shown the values of MBP**::** PP1β normalized against their respective GST baits and the ratio of these values relative to WT GST:: $MKLP1_{620-858}$.

Supplementary Table S1. List of the proteins showing differential abundance at the midbody after CIT-K depletion. Proteins that were significantly less or more abundant (*p* value < 0.01) in CIT-K siRNA midbodies are listed. The corresponding normalized logarithmic ratios and corrected p-values from experiment 1 and experiment 2 are shown. Proteins shaded in blue were underrepresented (negative logarithmic ratios) after CIT-K depletion. Proteins shaded in red were overrepresented (positive logarithmic ratios).

Gene	Protein	log_2 ratio exp. 1	log_2 ratio exp. 2	*p*-value exp. 1	*p*-value exp. 2
CIT-K	Citron kinase	-2.69	-2.47	$2x10^{-45}$	$1.4x10^{-25}$
PC	Pyruvate carboxylase, mitochondrial	-0.80	-0.86	$3x10^{-9}$	$3.9x10^{-4}$
ASS1	Argininosuccinate synthase	-0.52	-0.63	$7.6x10^{-5}$	$5.5x10^{-4}$
FLNB	Filamin B	-0.50	-0.56	$1.2x10^{-4}$	$2.1x10^{-3}$
TIMM44	Mitochondrial import inner membrane translocase subunit TIM44	-0.40	-1.04	$1.4x10^{-3}$	$1.82x10^{-5}$
PPIB	Peptidyl-prolyl cis-trans isomerase B	-0.37	-0.57	$3.1x10^{-3}$	$1.8x10^{-3}$
AURKA	Aurora kinase A	0.45	0.69	$5x10^{-3}$	$2.6x10^{-4}$
CKAP2	Cytoskeleton-associated protein 2	0.45	0.67	$5x10^{-3}$	$3.7x10^{-4}$
PTPRF	Receptor-type tyrosine-protein phosphatase F	0.62	1.19	$2.3x10^{-3}$	$9.71x10^{-10}$
TPX2	Targeting protein for Xklp2	0.71	0.75	$4.3x10^{-6}$	$6.65x10^{-5}$
HNRNPH3	Heterogeneous nuclear ribonucleoprotein H3	0.83	0.97	$3.2x10^{-5}$	$5.47x10^{-7}$
KIFC1	Kinesin-like protein KIFC1	0.87	0.55	$1.5x10^{-5}$	$3.3x10^{-3}$

Supplementary Table S2. List of the serine/threonine phosphatases present in the midbody interactome. The baits are listed in the top row and the phosphatases in the far left column. Protein names are according to the UniProt database. Member of the PP1 family are shaded in green, while members of the PP2 family are shaded in red. The Mascot score (Score) and number of peptides (Pept) identified in each AP-MS experiment are indicated. The far-right column indicates whether the phosphatase was identified in the midbody proteome.

Baits	Anillin	Aurora B	CHMP4B	CHMP4C	CIT-K	ECT2	KIF14	KIF20A	KIF23/ MKLP1	PRC1	Proteome
PPP1CA	Score 183 Pept 5			Score 244 Pept 6	Score 1392 Pept 21	Score 400 Pept 9	Score 658 Pept 10	Score 303 Pept 8	Score 75 Pept 3	Score 1004 Pept 16	Yes
PPP1CB					Score 1312 Pept 19	Score 342 Pept 8	Score 85 Pept 1	Score 253 Pept 6		Score 963 Pept 14	No
PPP1CC	Score 267 Pept 9	Score 117 Pept 1	Score 302 Pept 6		Score 1355 Pept 20	Score 338 Pept 8	Score 690 Pept 12	Score 407 Pept 6	Score 68 Pept 2	Score 1067 Pept 19	Yes
PPP1R9A	Score 235 Pept 3		Score 120 Pept 2	Score 83 Pept 3		Score 254 Pept 4	Score 67 Pept 1	Score 48 Pept 1		Score 78 Pept 1	No
PPP1R9B	Score 237 Pept 5		Score 285 Pept 6			Score 340 Pept 7	Score 273 Pept 5	Score 94 Pept 1	Score 98 Pept 2		No
PPP1R12A (MYPT1)	Score 185 Pept 2		Score 197 Pept 3	Score 60 Pept 5	Score 572 Pept 6	Score 363 Pept 11	Score 855 Pept 15	Score 152 Pept 5		Score 564 Pept 13	Yes
PPP1R12B	Score 87 Pept 1						Score 83 Pept 1				No
PPP1R12C							Score 346 Pept 4	Score 87 Pept 1		Score 56 Pept 1	No
PPP1R18	Score 96 Pept 1		Score 128 Pept 1		Score 85 Pept 1	Score 232 Pept 4	Score 400 Pept 8	Score 201 Pept 7			No
PPP1R13L							Score 101 Pept 2	Score 222 Pept 2			Yes
PPP2CA				Score 38 Pept 1							No
PPP2R5A				Score 24 Pept 3	Score 107 Pept 2		Score 34 Pept 1			Score 98 Pept 2	Yes
PPP2R1B										Score 46 Pept 1	Yes
PPP3CA			Score 61 Pept 1			Score 63 Pept 1					No
MPRIP	Score 1358 Pept 23		Score 390 Pept 6	Score 43 Pept 3	Score 66 Pept 1	Score 179 Pept 6	Score 528 Pept 10	Score 432 Pept 5	Score 85 Pept 2		No
CDC25A		Score 48 Pept 9			Score 39 Pept 3					Score 35 Pept 1	No
PGAM5	Score 359 Pept 11		Score 75 Pept 2	Score 108 Pept 4	Score 61 Pept 4	Score 74 Pept 3	Score 430 Pept 13	Score 372 Pept 13	Score 171 Pept 6	Score 101 Pept 2	Yes

Supplementary Video Captions

Supplementary Video S1.

This movie shows the different focal planes (z sections at 0.25 μm step size) of the tubulin immuno-staining of the late telophase control cell depicted in Fig. S5A (left bottom panels).

Supplementary Video S2.

This movie shows the different focal planes (z sections at 0.25 μm step size) of the tubulin immuno-staining of the late telophase *MYPT1* siRNA cell depicted in Fig. S5A (right bottom panels).

Supplementary Video S3.

This movie shows the 3D reconstruction of the tubulin immuno-staining of the late telophase control cell depicted in Fig. S5A (left bottom panels).

Supplementary Video S4.

This movie shows the 3D reconstruction of the tubulin immuno-staining of the late telophase *MYPT1* siRNA cell depicted in Fig. S5A (right bottom panels).

Supplementary Video S5.

This movie shows GFP::tubulin and histone H2B::mCherry dynamics in a control cell that successfully completed cytokinesis; see Fig. 3A for details. Cells were treated with dsRNA directed against a random sequence (control) for 30 hours before start filming. See Figure 3A for details. All sequences were captured at 2 min intervals. Playback rate is 5 frames per second (FPS).

Supplementary Video S6.

This movie shows GFP::tubulin and histone H2B::mCherry dynamics in an *MYPT1* siRNA cell. Note the long and thin central spindle that snaps after more than 2 hours after anaphase onset; see Fig. 3A for details. Cells were treated with dsRNA directed against *MYPT1* for 30 hours before start filming. All sequences were captured at 2 min intervals. Playback rate is 5 frames per second (FPS).

Supplementary Video S7.

This movie shows GFP::tubulin and histone H2B::mCherry dynamics in an *MYPT1* siRNA cell. In this cell, a long and thin central spindle forms after completion of furrow ingression, but there is no abscission and cytokinesis ultimately fails forming a single binucleate cell. Cells were treated with dsRNA directed against *MYPT1* for 30 hours before start filming. All sequences were captured at 2 min intervals. Playback rate is 5 frames per second (FPS).

Supplementary Video S8.

This movie shows GFP::tubulin and histone H2B::mCherry dynamics in an *MYPT1* siRNA cell. This cell shows abnormal contractility during furrow ingression, fails to properly assemble the central spindle and consequently cytokinesis fails prior to midbody formation. Cells were treated with dsRNA directed against *MYPT1* for 30 hours before start filming. All sequences were captured at 2 min intervals. Playback rate is 5 frames per second (FPS).

Supplementary Data Captions

Supplementary Data S1. (separate file)

Excel file listing the proteins identified by MS from the pull downs of CIT-K::AcGFP expressing cells at different cell cycle stages (see Fig. 1A, B). Each worksheet contains the results for a specific cell

cycle stage, i.e., S phase, metaphase and telophase. Non-specific binding proteins were removed by filtering each dataset against the corresponding dataset obtained from AP-MS experiments using HeLa cells expressing GFP alone at the same cell cycle stage (see Materials and Methods).

Supplementary Data S2. (separate file)

Excel file listing the proteins identified in the SILAC experiments (Fig. 1C to E) and the relative quantification analysis described in Materials and Methods.

Supplementary Data S3. (separate file)

Excel file listing the proteins identified by MS from the pull downs of telophase HeLa cells expressing the ten different baits indicated in Table S2. Each worksheet contains the results for a specific bait. Non-specific binding proteins were removed by filtering each dataset against the corresponding dataset obtained from AP-MS experiments using telophase HeLa cells expressing GFP alone (see Materials and Methods). The MS data for Flag::CHMP4C are from our previous study[2].

Supplementary Data S4. (separate file)

Excel file listing the proteins identified in the midbody proteome and interactome along with their respective gene names and GO terms. The proteins shared between the two datasets and the ones specific for each dataset are shown in separate worksheets.

Supplementary Data S5. (separate file)

Excel file showing the results of the GO enrichment analyses of the midbody proteome and of the midbody interactome in two separate worksheets.

References

1 Edgar, R. C. MUSCLE: multiple sequence alignment with high accuracy and high throughput. *Nucleic Acids Res* **32**, 1792-1797, doi:10.1093/nar/gkh340 (2004).

2 Capalbo, L. *et al.* Coordinated regulation of the ESCRT-III component CHMP4C by the chromosomal passenger complex and centralspindlin during cytokinesis. *Open Biol* **6**, doi:10.1098/rsob.160248 (2016).